



Full length article



Fumarate reductase drives methane emissions in the genus *Oryza* through differential regulation of the rhizospheric ecosystem

Jia Hu^{a,b,1}, Girma Bedada^{b,1}, Chuanxin Sun^b, Choong-Min Ryu^c, Anna Schnürer^d, Pär K. Ingvarsson^{b,*}, Yunkai Jin^{a,b,**}

^a College of Agronomy, Hunan Agricultural University, Changsha 410128, China

^b Department of Plant Biology, Uppsala BioCenter, Linnean Centre for Plant Biology, Swedish University of Agricultural Sciences (SLU), PO Box 7080, SE-75007 Uppsala, Sweden

^c Molecular Phytobacteriology Laboratory, Infectious Disease Research Center, KRIBB, Daejeon 34141, South Korea

^d Department of Molecular Sciences, Uppsala BioCenter, Swedish University of Agricultural Sciences (SLU), PO Box 7015, SE-75007 Uppsala, Sweden

ARTICLE INFO

Handling Editor: Adrian Covaci

Keywords:

Methane emissions
Oryza evolution
 Rhizosphere ecosystem
 Electron transport
 Fumarate reductase

ABSTRACT

The emergence of waterlogged *Oryza* species ~15Mya (million years ago) supplied an anoxic warm bed for methane-producing microorganisms, and methane emissions have hence accompanied the entire evolutionary history of the genus *Oryza*. However, to date no study has addressed how methane emission has been altered during *Oryza* evolution. In this paper we used a diverse collection of wild and cultivated *Oryza* species to study the relation between *Oryza* evolution and methane emissions. Phylogenetic analyses and methane detection identified a co-evolutionary pattern between *Oryza* and methane emissions, mediated by the diversity of the rhizospheric ecosystems arising from different oxygen levels. Fumarate was identified as an oxygen substitute used to retain the electron transport/energy production in the anoxic rice root, and the contribution of fumarate reductase to *Oryza* evolution and methane emissions has also been assessed. We confirmed the between-species patterns using genetic dissection of the traits in a cross between a low and high methane-emitting species. Our findings provide novel insights on the evolutionary processes of rice paddy methane emissions: the evolution of wild rice produces different *Oryza* species with divergent rhizospheric ecosystem attributing to the different oxygen levels and fumarate reductase activities, methane emissions are comprehensively assessed by the rhizospheric environment of diversity *Oryza* species and result in a co-evolution pattern.

1. Introduction

Methane is the second most important greenhouse gas after carbon dioxide, and by weight, the comparative impact of methane is 28 times greater than carbon dioxide (EPA, 2020). Methane emissions have risen tenfold in the past decade due to increasing agricultural activity (Sau- nois et al., 2020), and rice paddies constitute ca. 7–17 % of the total methane emitted from anthropogenic sources (IPCC, 2013). Thus, ef- forts to mitigate methane emissions from rice paddies have been in focus over the past decades (Denier Van Der Gon et al., 2002; Su et al., 2015; Jiang et al., 2017; Hu et al., 2023, 2024) even if the mechanisms behind methane emissions remain poorly understood. To improve the

mitigation of methane emissions, it is of critical importance to further understand the mechanisms controlling methane emissions.

The genus *Oryza* arose around 15Mya (million years ago) (Ammiraju et al., 2008) and includes 21 wild species (Khush, 1997; Vaughan et al., 2003), encompassing all 10 recognized genome types (AA, BB, BBCC, CC, CCDD, EE, FF, GG, HHJJ and HHKK), all growing in highly diverse environments. Genomic changes have led to the diversification of the genus around the world, and modern cultivated rice (*Oryza sativa*) was first domesticated approximately 9000 years ago (Fornasiero et al., 2022). Unlike the evolution of other major food crops, such as maize and wheat, rice did not undergo drastic morphological or genome modifi- cations during domestication, which makes it challenging to trace the

* Corresponding author.

** Corresponding author at: Department of Plant Biology, Uppsala BioCenter, Linnean Center for Plant Biology, Swedish University of Agricultural Sciences, SE-750 07 Uppsala, Sweden.

E-mail addresses: par.ingvarsson@slu.se (P.K. Ingvarsson), yunkai.jin@slu.se (Y. Jin).

¹ Equal contributors.

<https://doi.org/10.1016/j.envint.2024.108913>

Received 27 May 2024; Received in revised form 17 July 2024; Accepted 24 July 2024

Available online 26 July 2024

0160-4120/© 2024 The Author(s). Published by Elsevier Ltd. This is an open access article under the CC BY license (<http://creativecommons.org/licenses/by/4.0/>).

evolution of important crop traits (Sang and Ge, 2007).

The *Oryza* root constitutes a highly anaerobic environment and the rhizosphere of rice has been identified as an independent ecosystem for microorganisms living in the vicinity of rice roots which is altered as the plant root systems develop and grow through the soil (Ma et al., 2022; Shenton et al., 2016). This ecosystem is mainly dependent on root metabolism and its exudates, and has been shown to differ widely among different *Oryza* accessions (Shenton et al., 2016; Shi et al., 2019; Wagner et al., 2016). Root exudates could alter the soil chemical environment, increase microbial metabolism, and/or change the composition of microbial communities (Waldo et al., 2019; Turner et al., 2020; Ding et al., 2022). Increased abundance of bacteria, e.g. *Chloroflexi*, *Firmicutes* and *Actinobacteria*, has been discovered in the rhizosphere of high methane emission rice varieties and this has been attributed to high carbohydrate secretion from root. This range of soil microorganism participate in decomposition pathways of C-containing substrates and provides end carbon sources to methanogens, i.e. acetate or CO₂/H₂ (Waldo et al., 2019; Ding et al., 2022; Määttä and Malhotra, 2024). Moreover, fumarate has been reported as one of the most important root exudates to regulate methane emissions in rice paddies (Jin et al. 2021). Fumarate is exuded by different plant species, including rice, and plays a role in plant–microbe interactions as it can be used as both a carbon source and as an electron transporter for microbial growth, such as members of genus *Geobacter*, which are well known key players for carbon cycling and have also been shown to perform the collaboration with methanogens (Yang et al., 2010; Lecomte et al., 2018; Li et al., 2023; Li and Zhou, 2020; Holmes et al., 2017). Thus, methane production is regulated by root exudates in rice paddies, and it is also known to differ between *Oryza* species (Wagner et al., 2016; Mauerer et al., 2018; King and Reeburgh, 2002). Elucidation of the evolutionary processes that have shaped methane emissions in the genus *Oryza* is therefore highly relevant to help mitigate methane emissions from rice cultivation.

Based on the earlier reports outlined above, we hypothesis that: 1) The ecosystem in the rhizosphere has co-evolved with different *Oryza* species and has diverged during *Oryza* evolution; 2) Methane emissions are related to composition of the rhizosphere community and hence to evolution within the genus *Oryza* evolution. To test our hypotheses, we performed phylogenetic analyses, rhizospheric ecosystem analyses and estimated methane emissions in two cultivated *Oryza* species (genome types AA) and five wild rice progenitors (genome types AA, GG, FF, BBCC, CCDD). To further evaluate our hypotheses, we also generated a segregating population by crossing a low and high methane-emitting rice species to assess the genetic basis of these traits and how these link to methane emissions. Our results demonstrate that methane emissions have co-evolved throughout the evolutionary history of the *Oryza* genus and that this has been mediated by the divergence of the rhizospheric ecosystems and through different fumarate reductase activities.

2. Materials and methods

2.1. Plant growth conditions and *Oryza* hybridization

Two cultivated *Oryza* species (genome type AA): *Oryza sativa* (*O. sativa*, including three Japonica varieties: Nipponbare (Nipp), Jiahua and Heijing 5, and two Indica varieties Huanghuazhan (HHZ) and Zaoxian) and *Oryza glaberrima* (varieties OG_113 and OG_126), and five wild progenitors *Oryza nivara* (genome type AA), *Oryza meyeriana* (genome type GG), *Oryza brachyantha* (genome type FF), *Oryza eichingeri* (genome type BBCC) and *Oryza alta* (genome type CCDD) were used in this study. All species were grown in a phytotron under the following conditions: 14 h of light (400 μmol photons m⁻² s⁻¹) at 30 °C, and 10 h of dark at 21 °C, with the humidity in the growth chambers set at 80 % for the entire growth period. All the experiments, except crossings, were performed during the stage before flowering as the different flowering

times and grain filling rates seen between different *Oryza* species, as well as among individuals from the F₂/F₃ population, will make the mechanisms involved even more complex.

A cross was performed between the low methane emission cultivar Heijing 5 (*Oryza sativa* L. ssp. Japonica) (Hu et al., 2023) and the high methane emission wild rice *O. nivara* as described by Poehlman and Sleper (Poehlman et al., 1999). The offspring from this cross were subsequently inbred for one generation in the phytotron under the conditions described above. Individuals from the segregating F₂ population were selected based on phenotype and inbred for one more generation. The F₂ generation plants were used for phenotypic and phylogenetic analyses and the F₃ generation plants, which displayed the same phenotype as their F₂ parents, were used for analyses of methane emissions, metabolomics, oxygen level and fumarate reductase activity.

2.2. Methane measurements

Sampling for methane emissions was performed as described before (Su et al., 2015; Hu et al., 2023, 2024). Briefly, in the phytotron, methane was collected 8 weeks after planting by covering individual rice plants with sealed plastic cylinders (diameter: 15 cm, height: 95 cm) for 15 min, starting at 2 p.m. Gas samples were taken from the head-space of the plastic cylinders using a syringe for two times and pooled in a sealed vial (10 ml). Emissions from at least six plants were sampled from each *Oryza* species or population. All samples were analysed using gas chromatography and the concentrations were calculated using an external standard curve derived from samples with known methane concentrations (10, 20, 250, 1000 and 5000 ppm). Methane flux calculation was done as described by Yang et al. (2012).

2.3. qPCR quantification of methanogenic communities

Quantification of methanogenic communities was performed as described in previous studies (Su et al., 2015; Hu et al., 2024). Rhizospheric soil samples were collected from pots with rice plants grown in the phytotron. The collection started at 2.00 p.m., and each sample was taken from a soil depth of five cm. Total genomic DNA was extracted from 500 mg of fresh rhizospheric soil samples according to protocols described in the FastDNA Spin Kit for soil (MP Biomedicals LLC, USA). All DNA samples were adjusted to same concentration and 1 μl DNA was used to perform quantitative real-time PCR (qPCR) with different microorganism-specific primers. All primers were initially assessed and had at least 90 % amplification efficiency and showing a single band of the expected size. Methanosaetaceae (Mst), Methanosarcinaceae (Msc), Methanobacteriales (MBT), Methanomicrobiales (MMB), Methanocella-specific (Met), total archaea (ARC), methanogens (MET) (Narihiro and Sekiguchi, 2011), methyl coenzyme M reductase (*mcrA*) (Jiang et al., 2022) and sulphite-reduction bacteria (*dsr*) (Foti et al., 2007) were targeted. Previously cloned 16sRNA gene fragments from different pure cultures of methanogens were used as standards (Hu et al., 2023; Narihiro and Sekiguchi, 2011; Westerholm et al., 2011). The standards for quantification of Methanotrophs (*mxoF*) and total bacteria were prepared using DNA extracted from soil and the qPCR programme for *mxoF* was 95 °C for 7 min, then 40 cycles of 40 s at 95 °C, 1 min at 60 °C and 40 s at 72 °C; for total bacteria was 95 °C for 7 min, then 40 cycles of 40 s at 95 °C, 1 min at 55 °C and 40 s at 72 °C. All the standards were set up with 8 different concentration series to build the standard curve and also ensure that the C_t value of all the DNA samples was in the range of the standard curve. The samples were analyzed on a Bio-Rad CFX qPCR machine (California, USA), and the results were calculated based on the formula from the standard curve. Primer sequences used for the qPCR experiments are listed in (Table S1).

2.4. Gene expression analysis by quantitative PCR (qPCR)

Roots from different *Oryza* species or populations were collected at 6

weeks after planting, starting at 2.00 pm. Nipponbare rice roots at different oxygen levels or with fumarate treatment were also sampled for gene expression analyses. Each sample was snap-frozen in liquid nitrogen and stored until further use. Total RNA was isolated using the Spectrum Plant Total RNA Kit (QIAGEN, Germany) according to the manufacturer's protocol. All the samples were treated with Dnase I (Sigma-Aldrich, USA) to remove trace amounts of DNA contamination. A total RNA of 1 µg was used as a template for the cDNA synthesis with the Quanta qScript cDNA synthesis kit (Quanta Biosciences) and 15 ng cDNA was used for qPCR analysis, using primers with at least 90 % amplification efficiency. The qPCR program was performed as previously described (Su et al., 2015; Hu et al., 2023). qPCR data was calculated with the comparative C_t method, and gene expression level was normalized using the housekeeping gene Ubiquitin10. All primers used are listed in Table S1.

2.5. Oxygen detection

Plants were sampled 4 weeks after planting and the collected roots were carefully rinsed 3 times with distilled water. Rinsed plants were incubated in 1 L bottles filled with fresh distilled water. After sealing with parafilm and wrapping with aluminum foil, bottles were put back into the growth chamber under the same growth conditions as described above. Oxygen concentrations was measured at regular intervals as needed with a MW600 PRO Dissolved Oxygen Meter (Milwaukee, EU) by inserting the detector into water at 5 cm depth and the water was being stirred during measurements. During the incubation period, distilled water with corresponded oxygen levels was refilled when the remaining water in the bottle was less than 500 ml. To produce the distilled water with the required oxygen levels, the nitrogen replacing method was used where pure nitrogen was first imported into the bottom of water in the bottle to replace the oxygen. Oxygen levels were then tracked by an oxygen meter every ten minutes.

2.6. Chemical components and metabolomic analysis

To analyse metabolites from the rhizosphere or from root samples, 100 mg freeze-dried rhizosphere or grinded root was dissolved in 8 ml methanol, vortexed well, and sonicated for 10 min at 50–60 Hz, and then vortexed again. The samples were centrifuged at 3000g for 10 min and the supernatant was transferred into a new 15 ml Falcon tube. The liquid was subjected to vacuum centrifugation overnight. Subsequently, 380 ml MilliQ water was added to the dried samples, vortexed well, sonicated for 10 min at 50–60 Hz, and vortexed again. After another centrifugation at 3000g for 10 min, 350 µl of the supernatant was transferred into a 1.5 ml Eppendorf tube together with an NMR analysis solution consisting of 50 µl D₂O, 30 µl Internal Standard (TPS, 5.8 mM), 20 µl MilliQ water, and 150 µl 0.4 M phosphate buffer (pH 7.0). After mixing well, 580 µl of the solution was used for NMR analysis, as described previously (Coulomb et al., 2015; Rohnisch et al., 2018). ¹H NMR spectra were acquired using a Bruker Avance III spectrometer. The spectrometer operated at 600 MHz and was equipped with a cryogenically cooled probe and autosampler. NMR spectra were recorded with a zgesgp pulse sequence (Bruker Biospin) (25 °C, 128 transients, 4 s relaxation delay, 65 536 data points and spectral width of 17 942).

For the specific compounds analysis, NMR files were opened with AMIX (version 3.9.7) and corresponding chemical content was calculated based on the standard value. For metabolomic analysis, NMR data were exported into Excel with AMIX (version: 3.9.7). During the export process, bucket width range of 0–9 ppm was selected and then cut into pieces with 0.01 ppm, positive intensity mode was used to scale the reference region from left (0.05 ppm region) to the right (−0.05 ppm). If any piece contained more than 50 % of values <0.0001, it was completely filtered out as noisy data. Exported data was then analyzed with SIMCA (version 17) using the PCA module. Data categorization and model validation were first analyzed. The raw data was then used to

perform volcano analysis (<https://huygens.science.uva.nl/VolcaNoseR/>) based on the values of Log₂ foldchange/−Log₁₀ (P-value < 0.05) to identify compounds showing significant differences.

2.7. RNA sequencing and phylogenetic analysis

Total RNA isolation from root samples for RNA-seq was performed as described above. The isolated RNA samples were quality controlled using an Agilent 2100 Bioanalyzer (Agilent, USA) and samples with RIN (RNA Integrity Number) values ≥ 7 were shipped to Novogen, UK for mRNA libraries construction and sequencing. The libraries were sequenced on the NovaSeq 6000 platform using a 2x150 bp paired-end sequencing configuration, resulting in approximately 12 G of raw data per sample. The raw reads were preprocessed using fastp v0.23.2 (Chen et al., 2018) to remove adapters, low-quality and short reads and mismatches correction. Finally, clean reads were used for all downstream analyses.

2.8. Phylotranscriptomics of rice species and population

Phylotranscriptomic trees of the rice species and the mapping population were constructed using Read2Tree v0.1.5 (Dylus et al., 2024) and IQTREE v2.2.2.2 (Minh et al., 2020) pipelines. For the *Oryza* species tree construction, gene markers (the orthologous matrix – OMA groups) for *Oryza sativa* subsp. *japonica*, *Brachypodium distachon* and *Hordeum vulgare* were selected from the OMA database (Altenhoff et al., 2024) using the marker gene export function (https://omabrowser.org/oma/export_markers/) with minimum species coverage of 0.65 (a total of 18,928 orthologous groups – OGs). For the rice mapping population tree construction, a total of 16, 801 OGs were obtained for *Oryza sativa* subsp. *japonica* and *Oryza sativa* subsp. *indica* with minimum species coverage of 0.80. After the reference dataset was created with OGs, raw RNA-seq libraries from all rice species and populations were mapped to the respective OGs using the Read2Tree workflow. Similarly, PacBio isoforms sequencing (Iso-Seq) generated from leaf, spike and root tissues of the diploid timothy grass (*Phleum nodosum*) were mapped to the OGs using the Read2Tree workflow. Finally, a concatenated multiple sequence alignment (MSA) consisting of 8,760,576 sites was generated and further trimmed using TrimAl v1.4.rev15 tool with 'automated1' trimming method, which kept 92.5 % of sites (656,153 sites removed) from the rice MSA. The MSA created for the mapping population was used without further trimming. To construct a phylogenetic tree from the trimmed or untrimmed MSA, IQTREE v2.2.2.2 was used after identifying the best-fitting substitution model (Kalyaanamoorthy et al., 2017) with 1,000 ultrafast bootstrap replicates (Hoang et al., 2018) (−m MFP −B 1000 −bnni).

2.9. Divergence time dating for *Oryza* species

To estimate the divergence times in the *Oryza* genus, the species tree and gene trees were first constructed using IQTREE from 18,928 concatenated OGs and the trimmed MSA (8.1 million sites) with the best-fitting substitution model. The inferred bootstrap consensus tree from 1,000 replicates, the trimmed MSA and the identified best-fit model were then used to estimate the divergence time using IQTREE. The divergence times were calibrated based on the most recent common ancestor between *B. distachon* and *H. vulgare* (33 Mya – million years ago), which was obtained from the TimeTree database v5 (Kumar et al., 2022) (<https://timetree.org/>). The constructed trees were visualized using TreeViewer tool v2.2.0 (Bianchini and Sánchez-Baracaldo, 2024).

2.10. Fumarate reductase activity assay

Fumarate reductase activity was performed as described in (Spinelli et al., 2021) with slight modifications. In brief, *Oryza* roots were sampled from pots in the phytotron, washed under running tap water

three times and then ground into fine powder using liquid nitrogen. 100 mg fresh root powder was added to 50 μ L re-suspension buffer (0.22 M Mannitol, 0.075 M Sucrose, 1 mM EDTA, 10 mM HEPES pH 7.4, and one complete Protease inhibitor tablet (Sigma)) and 450 μ L SDH activity assay buffer (27.5 mM KH₂PO₄ pH 7.4, 1.1 mM CoQ-10 (Sigma), 3.5 g/L BSA), and then homogenized ten times. The homogenate solution was pre-incubated at 30 °C for 10 min. Fumarate reduction reactions were initiated by adding NADH to a final concentration of 1 mM and fumarate to a final concentration of 10 mM. The same substrate without fumarate addition was used as a control. Reactions were performed at 30 °C for 1 h. Samples were mixed well and centrifuged at 16,000g for 10 min at 4 °C and 370 μ L supernatants were mixed with NMR reaction buffer as described above and analyzed by NMR for identification of produced succinate. The difference in succinate between the fumarate addition reaction and the same substrate without fumarate addition was used to calculate fumarate reductase activity. The data was not used for further analysis if the difference was negative.

2.11. NAD⁺/NADH analysis

Fresh root powder was used for the NAD⁺/NADH extraction and analysis according to protocols provided in the NAD/NADH Quantification kits (SIGMA-ALDRICH, Cat. No: MAK037). Briefly, 30 mg fresh root powder was added to 400 μ L of NADH/NAD Extraction Buffer and homogenized for ten times. The homogenate was then centrifuged at 14,000 rpm for 5 min, and supernatant was transferred into a labeled tube. To detect total NADH and NAD (NAD total), 50 μ L of the extracted samples were transferred in duplicate into a 96 well plate.

To detect NADH, NAD must be decomposed before the reaction. NAD was decomposed by aliquoting 200 μ L of the extracted samples into microcentrifuge tubes and heated to 60 °C for 30 min in a heating block. Samples were cooled on ice and then centrifuged at 12,000g for 2 min at 4 °C to remove any precipitates. 50 μ L of the NADH solution were also transferred in duplicate into the same 96 well plate. A Master Reaction Mix was set-up with NAD Cycling Buffer and NAD Cycling Enzyme Mix (98 μ L+2 μ L) and 100 μ L of the Master Reaction Mix was added to each well. The samples were mixed well by pipetting and reactions were incubated for 5 min at room temperature to convert NAD to NADH. Finally, 10 μ L of NADH Developer was added into each well and then incubated at room temperature for 1 h and then stopped by adding 10 μ L of Stop Solution into each well and mixing well. Absorbance was measured at 450 nm and the calculation of NADH and NAD total were performed as described by the kit. During the analysis, 0 (blank), 20, 40, 60, 80, and 100 pmole per well standards were set up to ensure that the absorbance measurements of all samples were in the range of the standards, and samples were not used for further analysis if the difference between the value of NAD total and NADH was negative.

2.12. Oxygen addition experiment

To check the effect of oxygen on fumarate reductase activity, oxygen was added to incubated rice roots. Briefly, rice roots were collected 4 weeks after planting and rinsed 3 times with distilled water. The rinsed rice roots were then incubated in a bottle with 500 ml distilled water for 2 days. During the incubation, fresh air was pumped into the water continuously with an air pump for the purpose of adding oxygen, and the same set up without air pumping was used as a control. Rice roots were harvested after two days for further analysis.

2.13. Data availability

All data are presented in the main article and [Supplementary Information](#). Results of statistical analyses are provided in source data provided with this paper. The original RNAseq data that support the findings in this study have been deposited and made publicly available in ENA, under accession number PRJEB74493.

3. Results

3.1. Methane emissions correlate with *Oryza* evolution

To reveal links between methane emissions and phylogeny in diverse *Oryza* species, we initially performed a phylotranscriptomic analysis using whole-transcriptome sequencing data generated from anaerobically grown root tissue. The phylotranscriptomics tree constructed directly from RNA-seq reads of all diploid and tetraploid *Oryza* species shows distinct phylogenetic distances that capture the evolution footprints of the genus *Oryza* (Fig. 1a). *O. glaberrima*, *O. nivara* and *O. meyeriana* were closely affiliated with *O. sativa*, while *O. brachyantha*, *O. eichingeri* and *O. alta* grouped in a separate clade (Fig. 1a). We then measured methane emissions in the different *Oryza* species. Notably, *O. sativa*, including both Indica and Japonica cultivars, emitted on average 3.47 mg m⁻² h⁻¹ methane. *O. nivara*, *O. glaberrima* and *O. meyeriana* emitted similar levels of methane (7.9, 6.8 and 6.2 mg m⁻² h⁻¹ respectively) while *O. brachyantha* emitted 9.7 mg m⁻² h⁻¹, *O. eichingeri* and *O. alta* emitted 17.0 and 32.5 mg m⁻² h⁻¹ methane, respectively (Fig. 1b). These results were in line with the abundance of methanogenic Archaea, as measured by qPCR, i.e. the copy number of methanogens was significantly lower in *O. sativa* compared with other *Oryza* species, and *O. eichingeri* and *O. alta* possessed the highest abundance of methanogens (Fig. S1). The correlation between methane emissions and species diversity within the genus *Oryza* (Fig. 1a, b) suggest that this pattern reflect co-evolution between rice and the rhizospheric community of methanogens.

Methane formation from rice paddies is controlled by rhizospheric compounds that provide carbon sources and electron/energy to the microbial community, including methanogens (Maurer et al., 2018; King and Reeburgh, 2002; Paterson, 2003; Liechty et al., 2020). To dissect and understand the consistent link between methane emissions and *Oryza* evolution, we conducted metabolomics analyses with samples from the rhizosphere and from rice root tissues. The results showed a remarkable diversity among different *Oryza* species. *O. glaberrima*, *O. nivara* and *O. meyeriana* shared similar metabolomics pattern and were close to *O. sativa*. *O. brachyantha*, with *O. eichingeri* and *O. alta* again showing clear separation from the other species, in line with their genetic distance from *O. sativa* (Fig. 1c). Furthermore, similar results were also discovered in the root metabolomic analysis (Fig. S2). Thus, phylogeny, methane emissions and rhizosphere metabolomics are all vary in concert among different *Oryza* species and the results therefore indicate that methane emissions are strongly correlated with phylogeny in *Oryza* and that this is mediated by rhizospheric metabolites.

3.2. Wild progenitors possess a more hypoxic rhizospheric environment

Oryza species grow on waterlogged land and metabolism both in root and surrounding soil is oxygen sensitive (Jiang et al., 2022). One potential explanation for the observed differences in belowground metabolism as well as methane emissions from the different *Oryza* species could be differences in rhizospheric oxygen levels. To further explore the underlying mechanisms driving the diversity in levels of methane emissions from the different *Oryza* species, the oxygen transport ability of roots was analyzed using plants collected four weeks after planting. When plants were incubated in fresh water, similar dynamics of oxygen levels were detected in all species. Oxygen was initially consumed by the plant until reaching a minimum level after which it increased to a low, but stable level (Fig. 2a). *O. sativa* displayed higher oxygen levels than the other *Oryza* species during the whole dynamic process. When comparing the final, stable oxygen levels, the species showed consistent results in line with the discussion above, that is, *O. sativa* retained significantly higher oxygen levels than other species with an equilibrium oxygen content of 2.39 mg/L. In contrast, *O. glaberrima*, *O. nivara* and *O. meyeriana* all contained similar but comparably lower oxygen level at equilibrium, falling in the range of 1.0–1.2 mg/L. Finally, the oxygen

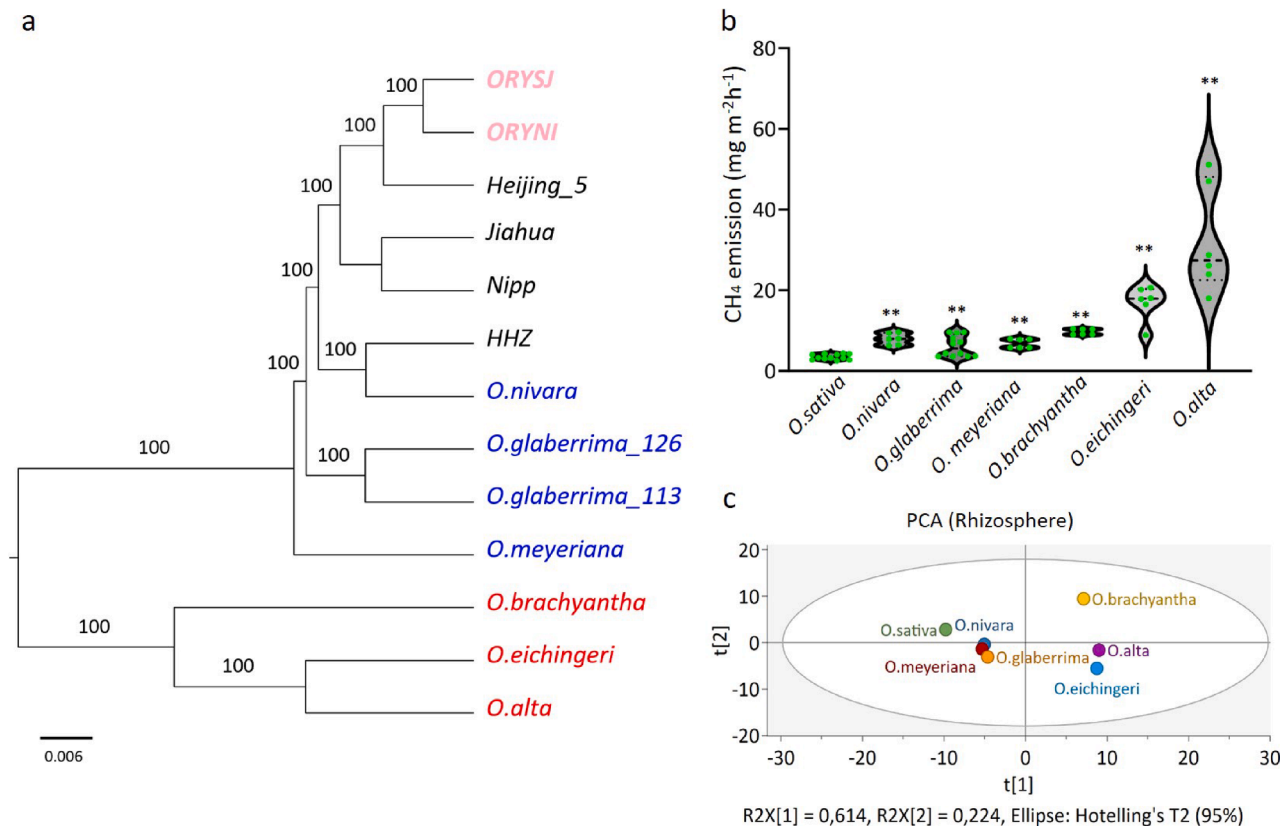


Fig. 1. Correlation between rice evolution and methane emissions a, A phylogeny of *Oryza* species. Two reference genomes – *O. sativa* subsp. Japonica (ORYSJ), *O. sativa* subsp. Indica (ORYNI) were used for orthologous groups selection from the OMA database. The scale bar represents branch length. b, Detection of methane emissions from different *Oryza* species. *O. sativa* was used as control. The green dots indicate data distribution. c, Principal component analysis (PCA) of the nuclear magnetic resonance (NMR) data from rhizosphere samples of different *Oryza* species. Average data from more than three replicates was used for the PCA analysis. A range of 0–9 ppm was selected and any piece contained more than 50 % of values < 0.0001 was completely filtered out as noisy data. One-way ANOVA was used to do the statistical analysis in b, $n \geq 3$, $**P \leq 0.01$, error bars show s.d. (For interpretation of the references to color in this figure legend, the reader is referred to the web version of this article.)

content in *O. brachyantha*, *O. eichingeri* and *O. alta* was 0.87 mg/L, 0.93 mg/L and 0.9 mg/L, respectively, lower than in all the other species. Theoretically, lower oxygen level indicates a higher root fermentation ability (Mustroph and Albrecht, 2003, 2010). To test this, roots were sampled from pots four weeks after planting to assess expression levels of genes responsible for the root fermentation process. As shown in Fig. 2b, the genes *ADH1*, *CYP2E*, *LDHA* and *LDHB* were selected (Miro and Ismail, 2013), and qPCR analyses of their expression indicate that gene expression levels were inversely correlated with oxygen content, i. e. wild progenitors with lower oxygen content showed higher gene expression levels, demonstrating a higher root fermentation ability in the wild *Oryza* progenitors (Fig. 2c). We further assessed levels of the fermentation products lactate and acetate (Miro and Ismail, 2013), and achieved results consistent with the gene expression analyses (Fig. S3), i. e. more lactate and acetate were detected in the rhizosphere of the wild *Oryza* progenitors. These results demonstrate the presence of a divergence in the oxygen environment in the rhizosphere across different *Oryza* species, which are thought to be a contributing factor to the corresponding profiles of rhizospheric metabolism and methane emissions observed.

In rice paddies, methane oxidizing microorganisms, methanotrophs, oxidize methane to CO₂ and consequently contributes to the final level of methane emissions (Macalady et al., 2002; Liu et al. 2016). This leads to the question if there is a positive link between lower oxygen levels in different wild *Oryza* species with a lower activity of methane oxidation and that this in turn results in higher methane emissions. To test this possibility, we assessed levels of various methanotrophs in the rhizosphere of the different *Oryza* species. Unexpectedly, higher abundance

of methanotrophs were observed in wild species, with *O. eichingeri* and *O. alta* containing the highest, indicating higher levels of methane oxidation in the *Oryza* progenitors having lower oxygen levels (Fig. S4). However, our results corroborate earlier reports that certain methanotrophs are overrepresented among the earliest diverged species of the *Oryza* genus (Tian et al., 2022). In addition to the methanotrophs, the proliferation of sulphate reducing bacteria (SRB) (Liu et al., 2018; Scholz et al., 2020), which competes for acetate with methanogenic microorganism, also affects the final level of methane emissions. To explore the involvement of SRB to any part of the methane emission process, the abundance of SRB was assessed. Similar to the high level of acetate observed in wild progenitors, a higher copy number of SRB was again discovered in wild *Oryza* species (Fig. S4). However, based on the methane production, the factors promoting methane emissions were comparably stronger than the potential of these factors for reducing the emission processes.

3.3. Fumarate sustains electron transport activity in hypoxic *Oryza* root

NAD⁺/NADH conversion plays an important role in maintaining electron transport during the fermentation process by accepting or donating electrons (Fig. 2b) (Tejedor-Sanz et al., 2022; Wang et al., 2021), and acetate produced in this process could be used by the rhizospheric methanogens for production methane as an end-product (Westerholm et al., 2019). The dynamic conversion of NAD⁺/NADH depends on the activity of the electron transport chain, and oxygen is usually used as a terminal electron acceptor to sustain its activity. The comparably faster oxygen consumption and higher fermentation ability

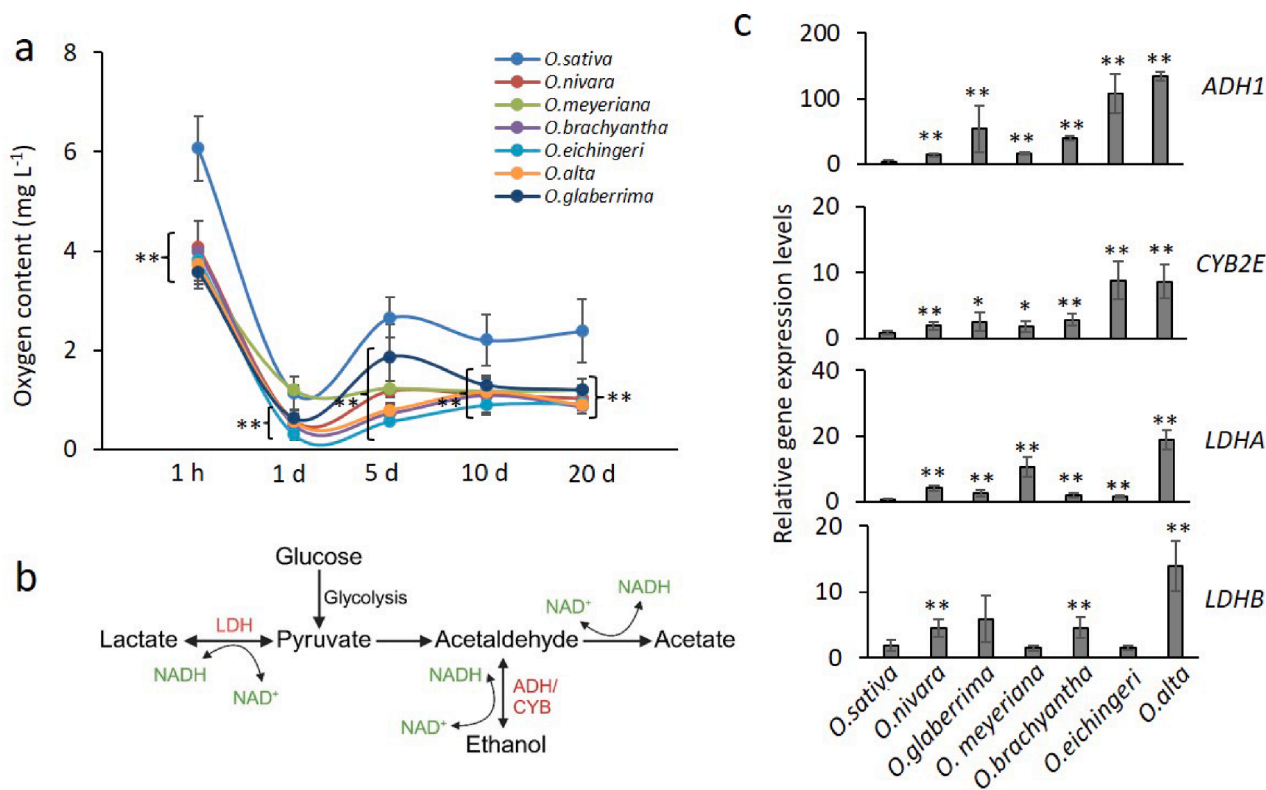


Fig. 2. Oxygen detection and fermentation analysis in rice root from different *Oryza* species. **a**, Rinsed rice root was incubated in fresh distilled water, and oxygen content in incubated water was measured at different time points. **b**, Schematic depiction of the fermentation pathway in anoxic rice roots²⁴. **c**, Expression levels of genes responsible for root fermentation reactions. T.TEST was used in **a** and **c** for the statistical analysis, $n \geq 3$, significance between *O. sativa* and other species is indicated with $**P < 0.01$ or $*P < 0.05$, error bars show s.d.

seen in the wild *Oryza* species indicates a highly dynamic conversion of NAD^+/NADH compared with *O. sativa*. To test this hypothesis, we estimated levels of NAD^+ and the ratio of NAD^+/NADH in *Oryza* roots. As expected, significantly higher levels of NAD^+ were detected in the root of the wild progenitors compared with *O. sativa*. *O. eichingeri* and *O. alta* contained the highest levels of NAD^+ (Fig. 3a). Furthermore, consistent results were also observed for the ratios of NAD^+/NADH , which is an indicator of the electron transport activity (Spinelli et al., 2021) (Fig. 3a). Thus, the dynamic of NAD^+/NADH conversion in the root of *Oryza* progenitors is higher than in the *O. sativa*, indicating a higher activity of the electron transport chain in wild *Oryza* species.

In mammals, fumarate can act as an electron acceptor and be reduced into succinate under hypoxia in order to sustain the activity of electron transportation (Spinelli et al., 2021). To further determine whether the higher dynamic conversion of NAD^+/NADH in wild *Oryza* species was also derived from reduction of fumarate, we performed a fumarate treatment with rice roots and observed a simultaneous enrichment of succinate and increase of the NAD^+ content and the NAD^+/NADH ratio (Fig. 3b, Fig. S5). A parallel experiment was also performed with the addition of oxantel, a fumarate reductase inhibitor which resulted in a significant decrease of both NAD^+ and the NAD^+/NADH ratio (Fig. S5b).

Fumarate could secrete into rhizosphere to regulate the metabolism of rhizospheric ecosystem, e.g. rice root secretes fumarate into rhizosphere to increase the abundance of carbon decomposition microorganism and methanogenic communities and regulate methane emissions (Jin et al., 2021). Compared with *O. sativa*, a significant accumulation of fumarate and succinate were observed in the rhizosphere of the wild species (Fig. 3c), certifying the existing of higher level of fumarate in the root of wild progenitors and more fumarate was secreted into rhizosphere from wild *Oryza* species, and thereby leading to higher metabolic and electron transport activity in the rhizospheric ecosystem.

These patterns were further supported by the comparative metabolome profiles, and we could identify many compounds that accumulated at significantly higher levels in the wild species than in *O. sativa* (Fig. 3c) and higher abundance of total bacteria in wild progenitors (Fig. S6). Hence, we conclude that the wild progenitors possess a comparably higher amount of fumarate or higher conversion activity between fumarate and succinate, which could sustain the dynamics of the NAD^+/NADH conversion and electron transport and meanwhile regulates the rhizosphere metabolic activity.

To study the correlation between rhizospheric electron transport and methane emissions, an inhibitor of complex 1 of the electron transport chain (Spinelli et al., 2021), rotenone, was added to rice plants growing in pots, which were then assessed for levels of methane emission. As shown in Fig. 3d, the addition of rotenone significantly inhibited methane emissions, indicating the importance of rhizospheric electron transport for maintaining methane emissions, and therefore further highlights the link between fumarate reduction and methane emissions.

3.4. Fumarate reductase contributes to the evolution of *Oryza* and selected *poideae* species

As reported, succinate dehydrogenase drives both the function of succinate oxidization (succinate dehydrogenase, *SDH*) and fumarate reduction (fumarate reductase, *Frd*) (Jardim-Messeder et al., 2017; Thauer et al., 1977). The presence of abundant succinate would indicate higher level of fumarate reductase activity. To test whether this hypothesis was true for our different *Oryza* species, we assessed fumarate reductase activities in the fresh root from the different *Oryza* species. As expected, higher fumarate reductase activities were observed in the wild progenitors while *O. sativa* displayed the lowest *Frd* activity (Fig. 4a). These results corroborate the observation of higher succinate levels and increased NAD^+/NADH activity that was also observed in the wild *Oryza*

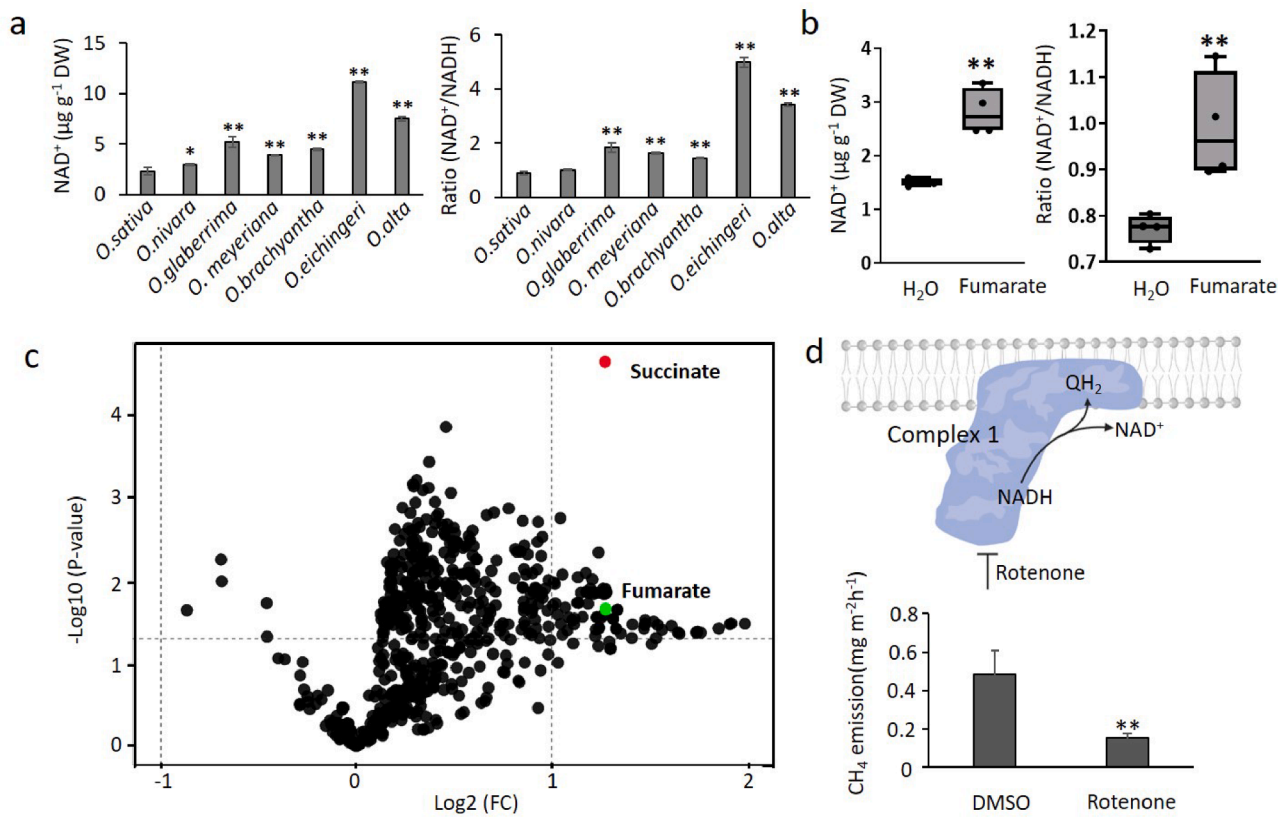


Fig. 3. Wild progenitors with lower oxygen content retain higher electron transport activity a, NAD⁺ and the ratio of NAD⁺/NADH in fresh roots from different *Oryza* species. *O. sativa* was used as a control. b, NAD⁺ content, the ratio of NAD⁺/NADH in rinsed Nipp root incubated with 10 mM fumarate in water for two days, rinsed Nipp root incubated only with water was used as control. The dots indicate data distribution. c, Metabolomic analysis of rhizosphere samples from different *Oryza* species. Succinate is marked in red and fumarate in green. A range of 0–9 ppm was selected and any piece contained more than 50 % of values < 0.0001 was completely filtered out as noisy data. P-value < 0.05 and Log₂(FC) ≥ 1 were used to identify compounds showing significant difference between *O. sativa* and the average data of all the wild progenitors. d, Methane emission levels after rotenone treatment in the pot. Rotenone inhibits complex 1 in the electron transport chain. DMSO was used as control to add into the pot. One-way ANOVA in c and T.TEST in a and d were used for the statistical analysis, n ≥ 3, **P<0.01 or *P<0.05, error bars show s.d. (For interpretation of the references to color in this figure legend, the reader is referred to the web version of this article.)

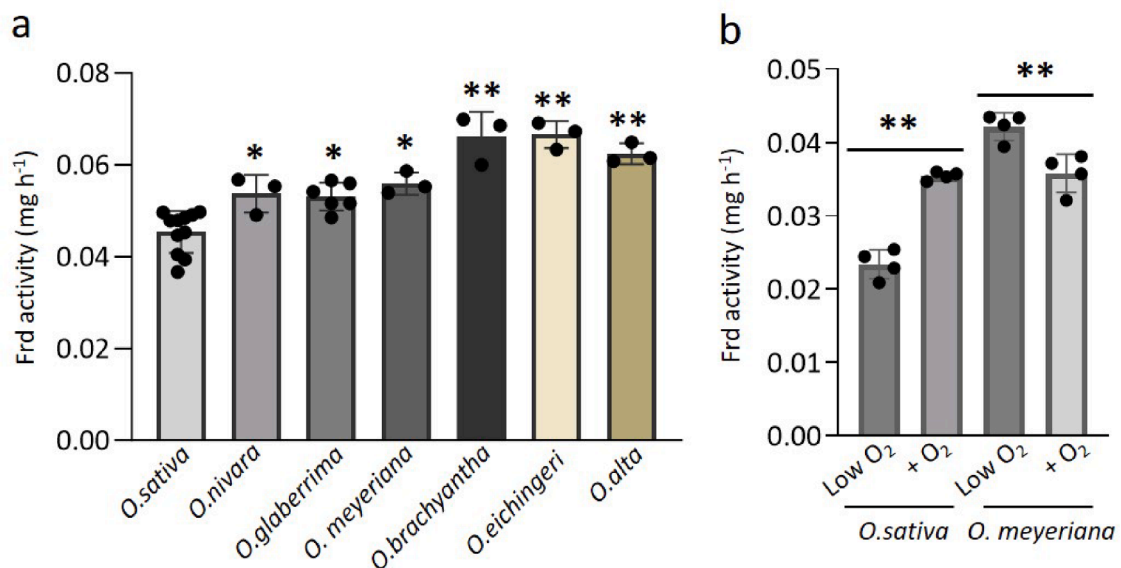


Fig. 4. Fumarate reductase (Frd) activity assay a, Fumarate reductase activity in the fresh rice root of different *Oryza* species. *O. sativa* was used as control. b, The reaction of fumarate reductase activity to different oxygen content in *O. sativa* and *O. meyeriana* respectively. Low O₂ was used as control. One-way ANOVA was used for statistical analysis in a and b, the dots indicate data distribution. n ≥ 3, **P<0.01 or *P<0.05, error bars show s.d.

species. To explain why different *Oryza* species possess diverse *Frd* activities, an oxygen addition experiment was further performed to assess the response of fumarate reductase to different oxygen levels. Notably, we observed an opposite effect of oxygen on fumarate reductase activity in *O. sativa* compared to the wild *Oryza* species, that is, low oxygen content inhibited fumarate reductase activity in the root of *O. sativa*. However, in the wild progenitors, fumarate reductase activity was higher when oxygen levels were low (Fig. 4b), which explains why wild progenitors possess high levels of fumarate reductase in the anoxic rhizosphere environment. More interestingly, when we checked the expression levels of different SDH subunit genes (Jardim-Messeder et al., 2017), we observed that all subunit genes (*SDH1-SDH4*) were inhibited by low oxygen in *O. sativa* (Fig. S7a). In wild rice, *SDH1* and *SDH4* were also inhibited by low oxygen, however, *SDH2* and *SDH3* were significantly induced in the low oxygen environment (Fig. S7a). Analysis of expression levels of the *SDH* genes in different *Oryza* species consistently showed higher expression levels of *SDH2* in the wild progenitors, while *SDH1*, *SDH3* and *SDH4* displayed the opposite trend (Fig. S7b). This result indicates that *SDH2* contributes to the adaptation of wild rice species to the hypoxic environments and highlights the existence of two different oligomeric isoforms of SDH in *O. sativa* and wild progenitors (Amino et al., 2000).

Hordeum and *Oryza* diverged more than 55 million years ago (Fig. S8a), with *Hordeum* having a closer evolutionary relationship with

timothy grasses (*Phleum* species) and *Brachypodium* (*B. distachyon*). Cultivated monocots, such as barley (*H. vulgare*), are generally known to be sensitive to waterlogging, while wild grasses (e.g. timothy and *Brachypodium*) are often better adapted to handle waterlogging environments (Fig. S8b) (Banach et al., 2009; Covshoff et al., 2016; Versluis et al., 2023). To further understand the contribution of fumarate reductase to monocots adapted to waterlogging conditions, fumarate reductase activity was measured in freshly harvested roots of rice, barley and different timothy grasses (*Phleum* species). The result showed lower fumarate reductase activity in barley compared to rice and timothy grasses (Fig. S8c), which underlines the contribution of *Frd* to the fermentative metabolism and evolution of flooding tolerance in grasses.

Additionally, fumarate could also be regarded as a valve that regulates fermentation reactions. The addition of fumarate to rice roots activates the expression of fermentation-related genes and enhances the production of lactate and succinate by over 5-fold (Fig. S9). The enriched organic acids could finally be reduced into methane and lead to an increase in methane emissions. Carbohydrates, organic acids and amino acids are the main forms of rice root exudates (Canarini et al., 2019). To assess the impact of different root exudates on the methanogenic communities, fumarate, acetate, succinate and sucrose were selected to perform the rice root treatments in the pot, and the abundance of methyl coenzyme M reductase (*mcrA*) (Jiang et al., 2022) was quantified to detect the abundance and/or activity of methanogens.

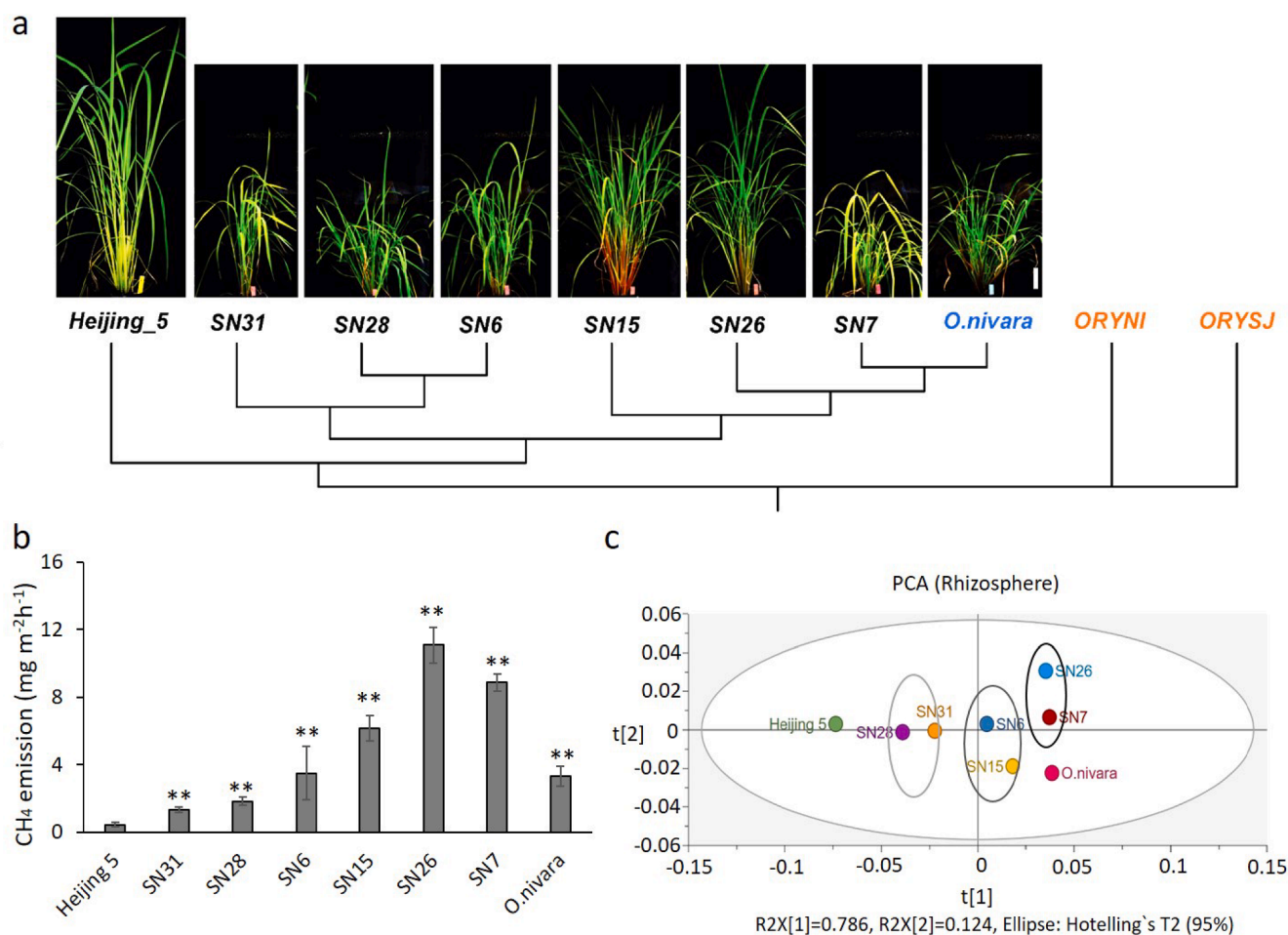


Fig. 5. Rapid evolution of different rice populations and corresponding methane emission analysis. **a**, Display of different rice populations after the phenotypic segregation, and corresponding phylogeny of rice F₂ population and their parental lines. ORYNI – *O. sativa* subsp. *indica* and ORYSJ – *O. sativa* subsp. *japonica* were the two reference genomes used for orthologous groups selection from the OMA database for use as outgroups, bar = 10 cm. **b**, Levels of methane emission of different rice populations. Heijjing 5 was used as control. **c**, Principal component analysis (PCA) of the nuclear magnetic resonance (NMR) data from rhizosphere samples of different rice populations. Average data from more than three replicates was used for the PCA analysis. A range of 0–9 ppm was selected and any piece contained more than 50 % of values < 0.0001 was completely filtered out as noisy data. T.TEST was used in **b**, n ≥ 3, **P<0.01, error bars show s.d.

Interestingly, the induction of fumarate on the proliferation of methanogens was more significant than other chemicals (Fig. S10), highlighting the importance of fumarate on methane regulation. All the results presented here demonstrate that fumarate/fumarate reductase have participated in the evolution of the rhizospheric ecosystems and hence regulate methane emissions in *Oryza* species.

3.5. The genetic architecture of methane emission

To further demonstrate the observed evolutionary patterns, we performed crosses between Heijing 5 (*O. sativa*) and *O. nivara*. Heijing 5 has been shown to be a low-methane rice variety (Hu et al., 2023, 2024), while *O. nivara* emits higher amounts of methane (Fig. 1b). A mapping population segregating for the different parental genetic backgrounds in the second generation (F₂) were created and, as expected, the F₂ mapping population show variation in phenotypic traits that differentiate the two parental lines (Heijing 5 and *O. nivara*). Six F₂ offspring were selected based on phenotype (Table S2) and presented using a phenotypic and phylotranscriptomic analysis (Fig. 5a). In the phenotypic analysis, stem color, plant height, seed shattering, and grain color were illustrated, as described in Table S2. Meanwhile, the phylotranscriptomic analysis also displayed different genetic distances among different F₂ progenies (Fig. 5a). We then tested the six F₃ progenies and the two parental lines for their pattern of methane emissions and observed that they showed variation in methane emission levels. Individuals from the F₂ population with closer genetic affinity to Heijing 5 (low methane emitter) emitted lower levels of methane while the opposite was observed for individuals from the F₂ population showing

greater genetic distances from Heijing 5 (Fig. 5b). The phylotranscriptome-based clustering in accordance with their methane emission patterns demonstrate that methane emission is regulated by several plant genes or gene families segregating between the two parental lines.

To understand if the segregating mapping population share the same mechanism as previously seen previously in the natural evolution of methane emissions among species, we again assessed oxygen levels, rhizospheric metabolism and fumarate reductase activity in the offspring from the mapping population (Fig. 5a). Notably, we observe a similar trend in oxygen levels and rhizospheric metabolism which were also consistent with the results from the phylotranscriptomic and methane emission assays (Fig. S11a and Fig. 5c). The results again demonstrated the co-evolution of rice plants and methane emissions. Furthermore, fumarate reductase activity assays showed the same trend with methane emissions, that is, higher methane-emitting individuals possess higher fumarate reductase activity (Fig. S11b). Thus, all our results highlight how rice evolution has influenced methane emissions.

4. Discussion

The rhizospheric area represents an ecosystem trait that depends on both root growth and secretion (Shenton et al., 2016; Paterson, 2003; Chang et al., 2022). Our analyses shows that metabolic profiles have diverged among different *Oryza* species, and it was possible to consistently classify species based on root traits and properties of the surrounding rhizosphere, demonstrating the direct effects of roots on the surrounding environment (Fig. 6). The strong link between metabolic

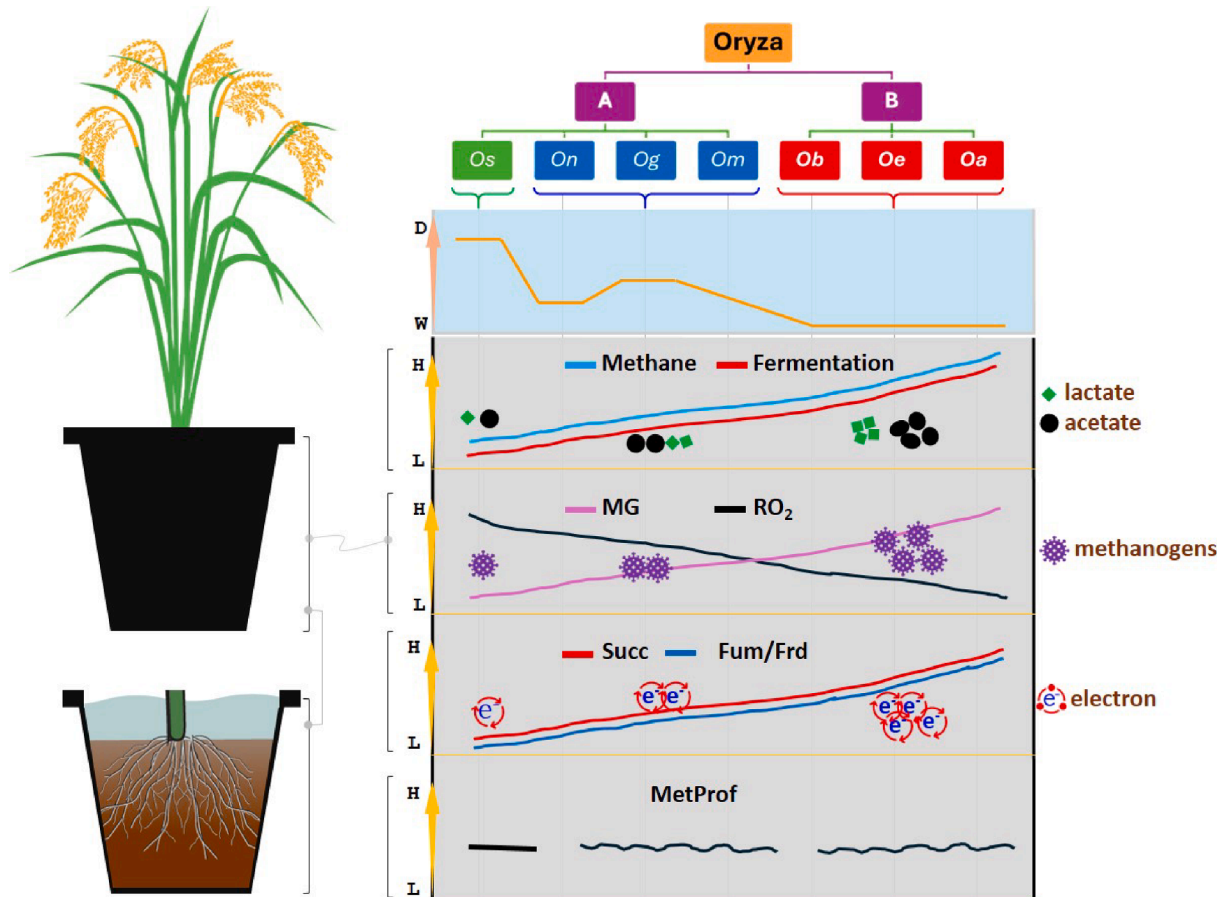


Fig. 6. Model depicting the co-evolution of *Oryza* species and methane emissions mediated by the rhizospheric eco-system. D: domestication (time); W: wild/Africa rice; H: high; L: Low; MG: methanogens; RO₂: rhizospheric oxygen level; Succ: succinate; Fum: fumarate; Frd: fumarate reductase activity; MetProf: metabolic profile; Os: *O. sativa*; On: *O. nivara*; Og: *O. glaberrima*; Om: *O. meyeriana*; Ob: *O. brachyantha*; Oe: *O. eichingeri*; Oa: *O. alta*.

profiles and methane emission pattern highlights that methane emissions are regulated by the plants. The tetraploid *Oryza* species emits significantly higher methane than the diploid species, perhaps due to the duplication of methane emission related genes or gene families in the tetraploid *Oryza*. Oxygen constitutes small part of the rhizospheric ecosystem, however the correlation between oxygen levels and metabolic profiles indicates its importance in the ecosystem, including the regulation of methane emissions, e.g. lower oxygen content in the wild progenitors results in higher methane emissions through altered rhizospheric metabolism.

Oxygen is known to maintain metabolic activity by acting as a terminal electron acceptor (Borisov and Verkhovsky, 2015). However, in the oxygen-limited rhizospheric ecosystem, metabolism and the activity of the electron transport chain is instead maintained by the use of fumarate as electron acceptor. Succinate dehydrogenase plays a central role in the mitochondrial metabolism as the most ancient enzyme catalysing both the forward (SDH) and reverse (Frd) conversion between fumarate and succinate (Jardim-Messeder et al., 2017; Thauer et al., 1977; Huang and Millar, 2013). The main role of succinate dehydrogenase in rice adaptation to waterlogging environments is reducing fumarate (Frd) into succinate in rice roots, especially in wild progenitors where lower oxygen level could induce fumarate reductase activity. Methane formation is a process of electron transport and carbon consumption. Based on our previous results (Jin et al., 2021), we assume that the main pathway for methane production from acetate in rice paddies is via syntrophic acetate-oxidising bacteria (SAOB) (Conrad and Klose, 2011; Yue et al., 2021), that oxidises acetate and transfers electrons, via direct electron transfer (DIET) or via H₂/CO₂ to methanogens (Yue et al., 2021). As an electron transfer, we speculate that fumarate reductase transfers electrons to fumarate to reduce fumarate to acetate as a characteristic metabolic end product via succinate and propionate as intermediate products (Jin et al., 2021). Acetate is subsequently oxidised into methane by SAOB via the transferring of electrons to methanogens. Thus, higher level of fumarate/fumarate reductase in wild *Oryza* ancestors increase electron transport to methanogens and organic carbon levels, and thereby increasing methane emissions.

Current diversity within the genus *Oryza* represents ca. 15 million years of independent evolution (Ammiraju et al., 2008). The analysis of a segregating mapping population created from a low and a high methane-emitting parental species not only mirrored the observed patterns of methane emissions among species in the genus, but also provide novel genotypes that can be used to develop low-methane rice varieties based on the rules of hybrid vigour and genetic segregation. The similar patterns we observe both among segregating offspring in the F₂ mapping population and among diverse species in the genus indicates a shared evolutionary pattern and suggest the co-evolution of methane emissions among different *Oryza* species.

O. glaberrima was domesticated around 3000 years ago while the domestication of *O. sativa* was initiated already 9000 years ago (Fornasiero et al., 2022). This could explain why *O. glaberrima* has a closer affinity to the wild rice species in both methane emission levels and root transcriptome profiles. Moreover, the lower levels of methane emissions we observe in *O. sativa* compared to *O. glaberrima* or other wild species indicates that rice domestication and subsequent improvement have facilitated the reduction of methane emissions (Tian et al., 2022). Methane emissions from African rice paddies are increasing fast, and the reduction of methane emissions through the domestication and diversification processes can be thus seen as one of the potential strategies for breeding of low-methane emitting African rice, and thereby significantly reducing rising methane emissions from the continuously expanding rice cultivation in African (Chen et al., 2024). The approach to create a population showing diversity in methane emissions in the segregating offspring as implemented in our study, combined with a whole-transcriptome sequencing method, can be utilized in rice breeding programs to screen and identify low-methane emitting rice genetic resources.

5. Conclusions and outlook

Using a phylotranscriptomic study and methane emission analyses, we uncovered a co-evolution pattern between evolution and speciation within the genus *Oryza* and methane emission levels, which attributes to the evolution of distinct rhizospheric ecosystems in the different *Oryza* species. Dissection of the methane emission traits using a mapping population derived from parental lines with different methane emission levels further confirmed these conclusions. Moreover, fumarate was identified as an oxygen substitute used to retain the electron transport/energy production in the anoxic rice root, and the different fumarate reductase activities have been discovered contributing to the evolution of diverse *Oryza* species and also methane emissions. Overall, rhizospheric oxygen levels and fumarate reductase activity in *Oryza* root are two important factors affecting rhizospheric ecosystem metabolism, e.g. fermentation activity and electron transport ability, and thus relate *Oryza* evolution with their ecological consequences, e.g. methane emissions. However, the main driving forces behind the decline of methane production during the transition from the wild species to the modern, domesticated varieties are still unknown and needs further study.

Our study provides a methodological exemplar for using distance hybridization between different *Oryza* species to breed novel low methane rice varieties with the purpose to reduce global methane emissions. Moreover, the lower levels of methane emissions from *O. sativa* compared to *O. glaberrima* indicates that rice domestication and subsequent improvement have facilitated the reduction of methane emissions. So cultivate the longer-time domesticated Africa rice varieties or introduce *O. sativa* into Africa can be thus seen as the potential strategies to significantly reduce rising methane emissions from the continuously expanding rice cultivation in Africa.

CRedit authorship contribution statement

Jia Hu: Writing – original draft, Resources, Methodology, Investigation, Formal analysis, Data curation, Conceptualization. **Girma Bedada:** Writing – review & editing, Software, Methodology, Investigation, Formal analysis, Conceptualization. **Chuanxin Sun:** Supervision, Funding acquisition, Conceptualization. **Choong-Min Ryu:** Writing – review & editing, Supervision, Methodology, Conceptualization. **Anna Schnürer:** Writing – review & editing, Supervision, Methodology, Investigation. **Pär K. Ingvarsson:** Writing – review & editing, Validation, Supervision, Resources, Project administration, Methodology, Funding acquisition, Conceptualization. **Yunkai Jin:** Writing – original draft, Validation, Supervision, Project administration, Methodology, Investigation, Conceptualization.

Declaration of competing interest

The authors declare that they have no known competing financial interests or personal relationships that could have appeared to influence the work reported in this paper.

Data availability

Data will be made available on request.

Acknowledgements

We thank International Rice Research Institute (IRRI) and Prof. Yves Vigouroux for providing the wild rice and *O. glaberrima* species; Simon Isaksson for methane analysis; Jens Sundström for the seed available application. This research was funded by Mr. Zheng Fang, Beijing Xianhe Transportation Technology Co. Ltd.; the Swedish Research Council for Environment, Agricultural Sciences and Spatial Planning (FORMAS; project no. 2020-01327).

Appendix A. Supplementary material

Supplementary data to this article can be found online at <https://doi.org/10.1016/j.envint.2024.108913>.

References

- Altenhoff, A.M., et al., 2024. OMA orthology in 2024: improved prokaryote coverage, ancestral and extant GO enrichment, a revamped synteny viewer and more in the OMA ecosystem. *Nucleic Acids Res.* 52, D513–D521.
- Amino, H., et al., 2000. Stage-specific isoforms of *Ascaris suum* complex. II: The fumarate reductase of the parasitic adult and the succinate dehydrogenase of free-living larvae share a common iron-sulfur subunit. *Mol. Biochem. Parasitol.* 106 (1), 63–76.
- Ammiraju, J.S., et al., 2008. Dynamic evolution of *oryza* genomes is revealed by comparative genomic analysis of a genus-wide vertical data set. *Plant Cell* 20 (12), 3191–3209.
- Banach, K., et al., 2009. Differences in flooding tolerance between species from two wetland habitats with contrasting hydrology: implications for vegetation development in future floodwater retention areas. *Ann. Bot.* 103 (2), 341–351.
- Bianchini, G., Sánchez-Baracaldo, P., 2024. TreeViewer: Flexible, modular software to visualise and manipulate phylogenetic trees. *Ecol. Evol.* 14 (2), e10873.
- Borisov, V.B., Verkhovsky, M.I., 2015. Oxygen as Acceptor. *EcoSal Plus* 6 (2).
- Canarini, A., et al., 2019. Root exudation of primary metabolites: mechanisms and their roles in plant responses to environmental stimuli. *Front. Plant Sci.* 10.
- Chang, J., van Veen, J.A., Tian, C., Kuramae, E.E., 2022. A review on the impact of domestication of the rhizosphere of grain crops and a perspective on the potential role of the rhizosphere microbial community for sustainable rice crop production. *Sci. Total Environ.* 10, 842:156706.
- Chen, Z., et al., 2024. African rice cultivation linked to rising methane. *Nat. Clim. Chang.* 14, 148–151.
- Chen, S., Zhou, Y., Chen, Y., Gu, J., 2018. fastp: an ultra-fast all-in-one FASTQ preprocessor. *Bioinformatics* 34, i884–i890.
- Conrad, R., Klose, M., 2011. Stable carbon isotope discrimination in rice field soil during acetate turnover by syntrophic acetate oxidation or acetoclastic methanogenesis. *Geochim. Cosmochim. Acta* 75, 1531–1539.
- Coulomb, M., Gombert, A., Moazzami, A.A., 2015. Metabolomics study of cereal grains reveals the discriminative metabolic markers associated with anatomical compartments. *Ital. J. Food Sci.* 27, 142–150.
- Covshoff, S., et al., 2016. C4 photosynthesis in the rice paddy: insights from the noxious weed *echinocloa glabrescens*. *Plant Physiol.* 170 (1), 57–73.
- Denier Van Der Gon, H.A., et al., 2002. Optimizing grain yields reduces CH₄ emissions from rice paddy fields. *PNAS* 99, 12021–12024.
- Ding, H., et al., 2022. Effect of microbial community structures and metabolite profile on greenhouse gas emissions in rice varieties. *Environ. Pollut.* 306, 119365.
- Dylus, D., et al., 2024. Inference of phylogenetic trees directly from raw sequencing reads using Read2Tree. *Nat. Biotechnol.* 42, 139–147.
- Fornasiero, A., Wing, R.A., Ronald, P., 2022. Rice domestication. *Curr Biol.* 32 (1), R20–R24.
- Foti, M., et al., 2007. Diversity, activity, and abundance of sulfate-reducing bacteria in saline and hypersaline soda lakes. *Appl. Environ. Microb.* 73, 2093–2100.
- Hoang, D.T., et al., 2018. UFBoot2: improving the ultrafast bootstrap approximation. *Mol. Biol. Evol.* 35, 518–522.
- Holmes, D.E., et al., 2017. Metatranscriptomic evidence for direct interspecies electron transfer between *Geobacter* and *Methanotherox* species in methanogenic rice paddy soils. *Appl. Environ. Microbiol.* 83 (9), e00223–e00317.
- Hu, J., et al., 2023. Characterisation of a low methane emission rice cultivar suitable for cultivation in high latitude light and temperature conditions. *Environ. Sci. Pollut. Int.* 40, 92950–92962.
- Hu, J., et al., 2024. A low-methane rice with high-yield potential realized via optimized carbon partitioning. *Sci. Total Environ.* 17, 920:170980.
- Huang, S., Millar, A.H., 2013. Succinate dehydrogenase: the complex roles of a simple enzyme. *Curr. Opin. Plant Biol.* 16 (3), 344–349.
- IPCC. Climate change 2013: The physical science basis. Working group I contribution to the fifth assessment report of the intergovernmental panel on climate change (2013).
- Jardim-Messeder, D., et al., 2017. Fumarate reductase superfamily: A diverse group of enzymes whose evolution is correlated to the establishment of different metabolic pathways. *Mitochondrion* 34, 56–66.
- Jiang, Y., et al., 2017. Higher yields and lower methane emissions with new rice cultivars. *Glob. Chang. Biol.* 23, 4728–4738.
- Jiang, M., et al., 2022a. Methane emission, methanogenic and methanotrophic communities during rice-growing seasons differ in diversified rice rotation systems. *Sci. Total Environ.* 842, 156781.
- Jiang, Y., Qi, M., Zhang, J., Wen, Y., Sun, J., Liu, Q., 2022b. Metabolomic Profiling Analysis of Physiological Responses to Acute Hypoxia and Reoxygenation in Juvenile Qingtian Paddy Field Carp *Cyprinus Carpio* Var *Qingtianensis*. *Frontiers in Physiology* 13, 853850.
- Jin et al., 2021. Reduced rice paddy methane emission through dual compound mechanism in novel cultivars. PREPRINT (Version 1) available at Research Square [<https://doi.org/10.21203/rs.3.rs-1087173/v1>] (2021).
- Kalyaanamoorthy, S., et al., 2017. ModelFinder: fast model selection for accurate phylogenetic estimates. *Nat. Methods* 14, 587–589.
- Khush, G.S., 1997. Origin, dispersal, cultivation and variation of rice. *Plant Mol. Biol.* 35, 25–34.
- King, J.Y., Reeburgh, W.S., 2002. A pulse-labeling experiment to determine the contribution of recent plant photosynthates to net methane emission in arctic wet sedge tundra. *Soil Biol. Biochem.* 34, 173–180.
- Kumar, S., et al., 2022. TimeTree 5: an expanded resource for species divergence times. *Mol. Biol. Evol.* 39, msac174.
- Lecomte, S.M., et al., 2018. Diversifying anaerobic respiration strategies to compete in the rhizosphere. *Front. Env. Sci.-Switz.* 6.
- Li, G., et al., 2023. Integrated microbiome and metabolomic analysis reveal responses of rhizosphere bacterial communities and root exudate composition to drought and genotype in rice (*Oryza sativa* L.). *Rice* 16, 19.
- Li, T., Zhou, Q., 2020. The key role of *Geobacter* in regulating emissions and biogeochemical cycling of soil-derived greenhouse gases. *Environ. Pollut.* 266 (Pt 3), 115135.
- Liechty, Z., et al., 2020. Comparative analysis of root microbiomes of rice cultivars with high and low methane emissions reveals differences in abundance of methanogenic archaea and putative upstream fermenters. *Msystems* 5.
- Liu, Y., et al., 2016. Responses of methanogenic and methanotrophic communities to elevated atmospheric CO₂ and temperature in a paddy field. *Front. Microbiol.* 24 (7), 1895. <https://doi.org/10.3389/fmicb.2016.01895>.
- Liu, P.F., Pommerenke, B., Conrad, R., 2018. Identification of Syntrophobacteraceae as major acetate-degrading sulfate reducing bacteria in Italian paddy soil. *Environ. Microbiol.* 20, 337–354.
- Ma, W., et al., 2022. Root exudates contribute to belowground ecosystem hotspots: a review. *Front. Microbiol.* 5, 13, 937940.
- Määttä, T., Malhotra, A., 2024. The hidden roots of wetland methane emissions. *Glob. Chang. Biol.* 30 (2), e17127.
- Macalady, J.L., et al., 2002. Population dynamics of type I and II methanotrophic bacteria in rice soils. *Environ. Microbiol.* 4 (3), 148–157. <https://doi.org/10.1046/j.1462-2920.2002.00278.x>.
- Maurer, D., Kiese, R., Kreuzwieser, J., Rennenberg, H., 2018. Processes that determine the interplay of root exudation, methane emission and yield in rice agriculture. *Plant Biol.* 20, 951–955.
- Minh, B.Q., et al., 2020. IQ-TREE 2: New Models and Efficient Methods for Phylogenetic Inference in the Genomic Era. *Mol. Biol. Evol.* 37, 1530–1534.
- Miro, B., Ismail, A.M., 2013. Tolerance of anaerobic conditions caused by flooding during germination and early growth in rice (*Oryza sativa* L.). *Front. Plant Sci.* 23, 4, 269.
- Mustroph, A., et al., 2010. Cross-kingdom comparison of transcriptomic adjustments to low-oxygen stress highlights conserved and plant-specific responses. *Plant Physiol.* 152 (3), 1484–1500.
- Mustroph, A., Albrecht, G., 2003. Tolerance of crop plants to oxygen deficiency stress: fermentative activity and photosynthetic capacity of entire seedlings under hypoxia and anoxia. *Physiol. Plant.* 117 (4), 508–520.
- Narihiro, T., Sekiguchi, Y., 2011. Oligonucleotide primers, probes and molecular methods for the environmental monitoring of methanogenic archaea. *J. Microbiol. Biotechnol.* 4, 585–602.
- Paterson, E., 2003. Importance of rhizodeposition in the coupling of plant and microbial productivity. *Eur. J. Soil Sci.* 54, 741–750.
- Poehliman, J.M., Sleper, D., 1999. *Breeding Field Crops*.
- Rohnisch, H.E., et al., 2018. AQUA: an automated quantification algorithm for high-throughput NMR-based metabolomics and its application in human plasma. *Anal. Chem.* 90, 2095–2102.
- Sang, T., Ge, S., 2007. Genetics and phylogenetics of rice domestication. *Curr. Opin. Genet. Dev.* 17 (6), 533–538.
- Saunio, M., et al., 2020. The global methane budget 2000–2017. *Earth Syst. Sci. Data* 12, 1561–1623.
- Scholz, V.V., Meckenstock, R.U., Nielsen, L.P., Risgaard-Petersen, N., 2020. Cable bacteria reduce methane emissions from rice-vegetated soils. *Nat. Commun.* 11 (1), 1878.
- Shenton, M., et al., 2016. Effect of wild and cultivated rice genotypes on rhizosphere bacterial community composition. *Rice (N Y)* 9 (1), 42.
- Shi, S., et al., 2019. Comparative analysis of the rhizomicrobiome of the wild versus cultivated crop: insights from rice and soybean. *Arch. Microbiol.* 201 (7), 879–888.
- Spinelli, J.B., et al., 2021. Fumarate is a terminal electron acceptor in the mammalian electron transport chain. *Science* 374 (6572), 1227–1237.
- Su, J., et al., 2015. Expression of barley SUSIBA2 transcription factor yields high-starch low-methane rice. *Nature* 523, 602–606.
- Tejedor-Sanz, S., et al., 2022. Extracellular electron transfer increases fermentation in lactic acid bacteria via a hybrid metabolism. *Elife* 11.
- Thauer, R.K., Jungermann, K., Decker, K., 1977. Energy conservation in chemotrophic anaerobic bacteria. *Bacteriol* 41, 100–180.
- Tian, L., et al., 2022. Comparison of methane metabolism in the rhizomicrobiomes of wild and related cultivated rice accessions reveals a strong impact of crop domestication. *Sci. Total Environ.* 803, 150131.
- Turner, J.C., et al., 2020. Getting to the root of plant-mediated methane emissions and oxidation in a Thermokarst bog. *JGR Biogeosciences* 125.
- Vaughan, D.A., Morishima, H., Kadowaki, K., 2003. Diversity in the *Oryza* genus. *Curr. Opin. Plant Biol.* 6 (2), 139–146.
- Verslues, P.E., et al., 2023. Burning questions for a warming and changing world: 15 unknowns in plant abiotic stress. *Plant Cell* 35 (1), 67–108.
- Wagner, M.R., et al., 2016. Host genotype and age shape the leaf and root microbiomes of a wild perennial plant. *Nat. Commun.* 7, 12151.
- Waldo, N.B., et al., 2019. Plant root exudates increase methane emissions through direct and indirect pathways. *Biogeochemistry* 145, 213–234.
- Wang, S., et al., 2021. bZIP72 promotes submerged rice seed germination and coleoptile elongation by activating ADH1. *Plant Physiol. Biochem.* 169, 112–118.

- Westerholm, M., et al., 2011. Quantification of syntrophic acetate-oxidizing microbial communities in biogas processes. *Env. Microbiol. Rep.* 3, 500–505.
- Westerholm, M., Dolfing, J., Schnürer, A., 2019. Growth Characteristics and Thermodynamics of Syntrophic Acetate Oxidizers. *Environ. Sci. Tech.* 53 (9), 5512–5520.
- Yang, S.H., et al., 2012. Methane and nitrous oxide emissions from paddy field as affected by water-saving irrigation. *Phys. Chem. Earth* 53–54, 30–37.
- Yang, T.H., Coppi, M.V., Lovley, D.R., Sun, J., 2010. Metabolic response of *Geobacter sulfurreducens* towards electron donor/acceptor variation. *Microb. Cell Fact.* 9.
- Yue, Y.N., et al., 2021. The fate of anaerobic syntrophy in anaerobic digestion facing propionate and acetate accumulation. *Waste Manag.* 124, 128–135.